JOURNAL OF VIROLOGY, Dec. 2009, p. 12462–12472 Vol. 83, No. 23
0022-538X/09/$12.00 doi:10.1128/JVI.01546-09

Inhibition of Protein Kinase R Activation and Upregulation of GADD34 Expression Play a Synergistic Role in Facilitating Coronavirus Replication by Maintaining De Novo Protein Synthesis in Virus-Infected Cells[▽]

Xiaoxing Wang,[1]† Ying Liao,[2]† Pei Ling Yap,[1] Kim J. Png,[1] James P. Tam,[2] and Ding Xiang Liu[1,2]*

Institute of Molecular and Cell Biology, Proteos, 61 Biopolis Drive, Singapore 138673,[1] and School of Biological Sciences, Nanyang Technological University, 60 Nanyang Drive, Singapore 637551,[2] Singapore

Received 26 July 2009/Accepted 15 September 2009

A diversity of strategies is evolved by RNA viruses to manipulate the host translation machinery in order to create an optimal environment for viral replication and progeny production. One of the common viral targets is the α subunit of eukaryotic initiation factor 2 (eIF-2α). In this report, we show that phosphorylation of eIF-2α was severely suppressed in human and animal cells infected with the coronavirus infectious bronchitis virus (IBV). To understand whether this suppression is through inhibition of protein kinase R (PKR), the double-stranded-RNA-dependent kinase that is one of the main kinases responsible for phosphorylation of eIF-2α, cells infected with IBV were analyzed by Western blotting. The results showed that the level of phosphorylated PKR was greatly reduced in IBV-infected cells. Overexpression of IBV structural and nonstructural proteins (nsp) demonstrated that nsp2 is a weak PKR antagonist. Furthermore, GADD34, a component of the protein phosphatase 1 (PP1) complex, which dephosphorylates eIF-2α, was significantly induced in IBV-infected cells. Inhibition of the PP1 activity by okadaic acid and overexpression of GADD34, eIF-2α, and PKR, as well as their mutant constructs in virus-infected cells, showed that these viral regulatory strategies played a synergistic role in facilitating coronavirus replication. Taken together, these results confirm that IBV has developed a combination of two mechanisms, i.e., blocking PKR activation and inducing GADD34 expression, to maintain de novo protein synthesis in IBV-infected cells and, meanwhile, to enhance viral replication.

Translation is a prime step for gene regulation in eukaryotic cells, especially when cells are stressed by various signals, including viral infection. Protein synthesis is globally limited in virus-infected cells, in many cases, by alteration of the phosphorylation status of the α subunit of eukaryotic initiation factor 2 (eIF-2α) at serine 51 (14). Phosphorylated eIF-2α has a higher affinity for eIF-2B, a guanine nucleotide exchange factor, than the nonphosphorylated form and binds to it tightly. Thus, eIF-2α is trapped and the formation of the 43S complex is impaired, resulting in the inhibition of global translation. Four kinases, namely, the heme-regulated inhibitor (7), the double-stranded-RNA (dsRNA)-activated protein kinase R (PKR) (54), the homologue of *Saccharomyces cerevisiae* protein kinase GCN2 (19), and the PKR-like endoplasmic reticulum eIF-2α kinase (PERK) (45), are known to phosphorylate eIF-2α under different circumstances (46). These kinases respond to different signals and play distinct roles in cells (9).

Among the kinase family, PKR is unique, as it is activated by dsRNA, often a by-product during virus replication, especially in cells infected with many RNA viruses (47). Therefore, PKR plays a critical defensive role in viral infection (44). PKR is expressed at a low level but is markedly induced at the transcriptional level by type I interferon (alpha/beta interferon) (15, 34). Binding to dsRNA induces autophosphorylation and dimerization of PKR, leading to the activation of the kinase (37). Following activation, PKR phosphorylates eIF-2α, resulting in the cessation of protein synthesis. Because of the deleterious effects of this cellular response on viral replication, many viruses have evolved mechanisms to countermeasure it (47). These mechanisms include a range of virus-encoded RNA-protein molecules directly interacting with PKR to block its activity (13, 21, 49, 53) and proteins binding to and sequestering dsRNA (16, 17). Some viruses can also inhibit the PKR activity by activating cellular inhibitors of PKR or cellular phosphatases (PPs) that dephosphorylate eIF-2α (5, 33). In addition, a recent report showed that translation of the late mRNA of alphaviruses was resistant to eIF-2α phosphorylation, as a highly stable RNA hairpin loop could bypass the requirement for a functional eIF-2α (51).

Dephosphorylation of eIF-2α is mediated by one of the major cellular protein PPs, PP1 (1, 52). PP1 regulates a number of cellular functions through interactions of the catalytic subunit (PP1c) with more than 50 known or putative regulatory partners (8). Most of these interacting proteins target PP1c to specific subcellular locations to carry out its enzymatic reactions. One well-established example is GADD34, a homologue of the mouse protein MyD116. GADD34 physically interacts with PP1c, leading to enhanced dephosphorylation of eIF-2α in vitro and in vivo (4, 42, 43). Induction of GADD34 by DNA

* Corresponding author. Mailing address: Institute of Molecular and Cell Biology, Proteos, 61 Biopolis Drive, Singapore 138673, Singapore. Phone: (65) 65869581. Fax: (65) 67791117. E-mail: dxliu@imcb.a-star.edu.sg.
† These authors contributed equally.
▽ Published ahead of print on 23 September 2009.

damage signals is well studied. More recently, its role in host-virus interaction has been emerging. For example, Kazemi et al. (18) reported that the E6 oncoprotein of papillomavirus type 18 associates with the GADD34/PP1 complex and mediates translational recovery. Vesicular stomatitis virus infection could induce GADD34 expression, which in turn suppresses viral replication in mouse embryo fibroblasts by dephosphorylation of TSC2 in the mTOR pathway (36).

Here, we report that infection of human and animal cell lines with infectious bronchitis virus (IBV), a group 3 coronavirus, suppresses eIF-2α phosphorylation and PKR activation and induces GADD34 expression. Inhibition of PP1 activity by okadaic acid (OA) and manipulation of the expression/activation of eIF-2α, PKR, and GADD34 in virus-infected cells either by knockdown with small interfering RNA or by overexpression of wild-type and mutant constructs showed that these viral regulatory strategies may play a synergistic role in facilitating coronavirus replication by maintaining de novo protein synthesis.

MATERIALS AND METHODS

Cells, viruses, antibodies, and reagents. Vero and HUH7 cells were maintained in Dulbecco's modified Eagle's medium supplied with 10% fetal bovine serum (FBS) and 1% penicillin-streptomycin (Gibco-BRL). H1299 cells and H1299 cells stably expressing *Renilla* luciferase (H1299-RL) were maintained in RPMI medium with 10% FBS and 1% penicillin-streptomycin. All cells were grown at 37°C and supplied with 5% CO_2. The medium for cells was replaced with FBS-free medium before and during virus infection. The H1299-RL stable cell line was made by overexpressing the *Renilla* luciferase gene in the pXJ41neo vector, and the positive cells were selected by use of G418 (Sigma-Aldrich).

A recombinant virus, IBV-Luc, was constructed by replacing open reading frame (ORF) 3a-3b with the firefly luciferase gene by using an in vitro ligation protocol (48). The virus was recovered from Vero cells electroporated with in vitro transcripts generated from the full-length IBV-Luc cDNA. All virus stocks were made in Vero cells by three repeated freeze-thaw cycles and kept at −80°C.

UV inactivation of the virus was performed by exposing IBV to shortwave UV radiation of 120,000 mJ/cm^2 at 254 nm of wavelength for 1 h within a CL-1000 cross-linker (UVP).

Polyclonal antibody against full-length IBV M and N proteins were raised in rabbits. Anti-β-tubulin was purchased from Sigma-Aldrich. Anti-eIF-2α and anti-phospho-eIF-2α (anti-p-eIF-2α; at Ser51) were from Cell Signaling. Anti-phospho-PKR (anti-p-PKR; at Thr451), anti-PKR, and anti-GADD34 were from Abcam. Anti-β-actin antibody was from Santa Cruz. Goat anti-rabbit horseradish peroxidase-linked secondary antibody and goat anti-mouse horseradish peroxidase-linked secondary antibody were from Dako.

OA from Sigma-Aldrich was dissolved in dimethyl sulfoxide (DMSO). For posttreatment, cells were infected by virus and incubated at 37°C for 1 h before the addition of OA at the indicated concentrations. Cells were then incubated for another 16 h before lysis. Lipofectamine 2000 was obtained from Invitrogen Life Technologies. DharmaFECT 2 was from Dharmacon.

Transient expression of plasmids in mammalian cells and establishment of the GADD34 knockdown cell line. Cells grown to 80% confluence were transfected with plasmid DNA by using Lipofectamine 2000 (Invitrogen) according to standard protocols. Cells were either lysed at 18 to 24 h posttransfection for immunoblotting or infected with virus at a multiplicity of infection (MOI) of 1 for another 16 to 18 h before lysis.

Vero cells were stably transfected with a GADD34 short hairpin RNA construct in the pSilencer 2.0 U6 vector (Ambion). Selection of positive clones was done in medium with G418.

Immunoblotting. Cells were washed with phosphate-buffered saline (PBS) and scraped with a rubber policeman. After centrifugation at 12,000 rpm for 1 min and removal of the supernatant, pellets were lysed in lysis buffer (50 mM Tris-Cl [pH 7.4], 150 mM NaCl, 1% SDS, 1% sodium deoxycholate) supplemented with protease inhibitor (Complete protease inhibitor cocktail from Roche). The samples were boiled for 5 min prior to sodium dodecyl sulfate-polyacrylamide gel electrophoresis (SDS-PAGE). The proteins were electrophoretically transferred to polyvinylidene difluoride membranes and immunoblotted according to the standard protocol, with appropriate antibodies at proper dilutions. The signals were detected using the ECL Plus chemiluminescence substrate kit (GE Healthcare).

Densitometry. The intensities of the bands were measured by a GS-710 calibrated imaging densitometer (Bio-Rad) and analyzed using Molecular Analyst computer software (Bio-Rad).

^{35}S metabolic labeling. Metabolic labeling was carried out according to methods described previously (22–27). Vero cells were infected with IBV or mock infected for different time periods. The medium was replaced with fresh Dulbecco's modified Eagle's medium lacking methionine-cysteine (Gibco), and cells were incubated at 37°C for 1 h. Cells were then pulse-labeled with 250 μCi/ml [^{35}S]Met-Cys labeling mixture (from GE Healthcare) for 2 h and then washed with PBS and lysed in SDS sample buffer. Protein extracts were subjected to SDS-PAGE, and radioactive proteins were visualized by autoradiography.

RNA extraction and Northern blotting. Cells were washed with PBS and lysed in TRIzol (Fisher Scientific), followed by the addition of 0.2 volumes of chloroform. After centrifugation at 12,000 rpm at 4°C for 10 min, the RNA fraction was transferred to a new tube and precipitated by 0.8 volumes of isopropanol. After centrifugation, RNA pellets were washed with 70% ethanol once and resuspended in RNase-free H_2O. Northern blotting was carried out according to a standard protocol (Roche). Briefly, RNA was separated on agarose gel and transferred to a positively charged nylon membrane. After prehybridization, a digoxigenin-labeled DNA probe was added after denaturation at 100°C for 5 min and immediate cooling on ice. The membrane was then probed with anti-digoxigenin antibody (Roche), and signals were detected using the CDP-star chemiluminescence substrate (Roche).

Luciferase reporter assay. Cells of 60 to 80% confluence grown on a 12-well plate were transfected with pXJ40F and pXJ40F-GADD34 plasmid DNAs by Effectene according to the manufacturer's instructions (Qiagen). At 12 h posttransfection, the medium was replaced with serum-free medium. Cells were infected with IBV-Luc at an MOI of 1 and were harvested for a luciferase reporter assay at the indicated time points (0 to 16 h) postinfection. The luciferase reporter assay was performed according to manufacturer's manual (Promega). Luminescence was measured with a TD-20/20 luminometer (Turner Designs).

H1299 cells of 90% confluence were transfected with pXJ40F vector pXJ40F-PKR, pXJ40F-K296P, pXJ40F-eIF2α, pXJ40F-S51D, or pXJ40F-S51A by use of Lipofectamine 2000 (Invitrogen) according to a standard protocol. Cells were then infected with IBV-Luc at an MOI of approximately 1 at 18 h posttransfection. Cells were lysed in 1× passive lysis buffer (PLB; Promega) at 18 h postinfection (h p.i.), and the luciferase assay was performed according to the manufacturer's manual (Promega).

H1299-RL cells seeded in a 12-well plate with 90 to 100% confluence were cotransfected with 0.5 μg reporter construct (pcDNA-FL) and 1 μg pXJ40F-PKR plus either 2 μg of plasmid encoding individual IBV proteins or 1 μg pXJ40F-NS1. At 18 h posttransfection, cells were lysed in 1× PLB and subjected to luciferase assay according to the manufacturer's protocol (Promega).

Plasmid construction. Full-length GADD34 was PCR amplified from cellular cDNAs and cloned into vector pXJ40F (with a Flag tag) under the control of a cytomegalovirus promoter. Similarly, full-length PKR and eIF-2α were PCR amplified from cellular cDNAs and cloned into pXJ40F, generating pXJ40F-PKR and pXJ40F-eIF-2α, respectively. PKR K296P and eIF-2α S51A and S51D mutants were constructed by site-directed mutagenesis (Stratagene). All IBV ORFs and nonstructural proteins (nsps) were obtained by reverse transcription-PCR from virus-infected cells by using appropriate primers and subsequently cloned into the pXJ40F vector.

RESULTS

A relatively steady level of de novo host cell protein synthesis was maintained in Vero cells infected with the coronavirus IBV. The effect of IBV infection on host cell protein synthesis was analyzed in two ways. First, Vero cells infected with IBV at an MOI of approximately 1 were harvested at 0, 8, 16, and 24 h p.i. Total proteins were separated by SDS-PAGE and visualized by direct staining with Coomassie blue. Similar levels of cellular protein synthesis were detected in mock- and IBV-infected Vero cells up to 24 h p.i. (Fig. 1, upper panel). At 16 and 24 h p.i., a protein band with an apparent molecular mass of approximately 32 kDa was detected in IBV-infected cells

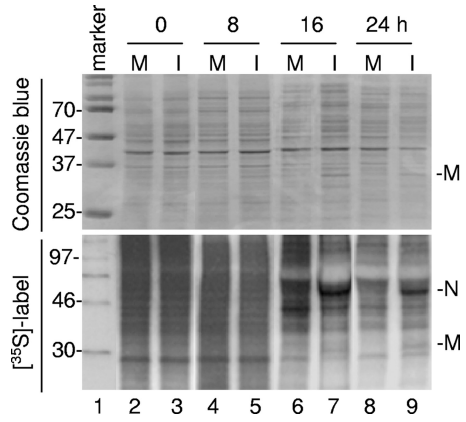

FIG. 1. Analysis of de novo protein synthesis in IBV-infected cells. IBV (I)- or mock (M)-infected Vero cell lysates harvested at 0, 8, 16, and 24 h p.i. were separated on an SDS–10% polyacrylamide gel and stained with Coomassie blue (upper panel). The lower panel shows metabolic labeling of IBV-infected cells. Vero cells infected with IBV at an MOI of approximately 2 were labeled with [^{35}S]Met-Cys for 2 h before harvest at 0, 8, 16, and 24 h p.i. Cell lysates were separated with 10% SDS-PAGE and subjected to autoradiography. IBV structural proteins M and N are indicated on the right of the gels. Lane 1 represents the protein ladder.

(Fig. 1, upper panel, lanes 7 and 9). It may represent the IBV membrane (M) protein. These results suggest that IBV infection did not significantly affect the steady level of host proteins up to 24 h p.i.

Metabolic labeling of IBV-infected cells with [^{35}S]Met-Cys was then carried out to study the kinetics of de novo protein synthesis in IBV-infected cells in a time course experiment. The infected cells were labeled with [^{35}S]Met-Cys at 0, 6, 14, and 22 h p.i. for 2 h and harvested. Cell lysates were prepared, and total proteins were separated with SDS-PAGE. The results showed that de novo host cell protein synthesis was not significantly affected up to 8 h p.i. (Fig. 1, lower panel). At 16 and 24 h p.i., two major proteins with molecular masses of approximately 32 and 46 kDa, representing the major IBV structural proteins M and nucleocapsid (N), respectively, were detected in IBV-infected cells (Fig. 1, lower panel) but not in mock-infected cells (Fig. 1, lower panel, lanes 6 and 8). It was noted that host cell protein translation was slightly reduced in both mock- and IBV-infected cells at late stages of the time course. This was probably due to prolonged incubation of cells in serum-free media. Nevertheless, the overall levels of protein synthesis in mock- and IBV-infected cells were comparable, which is consistent with previous studies (23, 24, 31, 38). These results demonstrate that de novo synthesis of host cell proteins is maintained in IBV-infected cells even at late stages of the infection cycle, although de novo synthesis of viral proteins becomes a more predominant event.

The expression and phosphorylation of eIF-2α were downregulated in IBV-infected Vero, H1299, and HUH7 cells, and IBV replication was inhibited by overexpression of the wild type and a phosphomimetic mutant of eIF-2α. It is well known that phosphorylation of eIF-2α leads to the loss of functional eIF-2α capable of binding to GTP and forming tertiary initiation complex with initiator tRNA^{Met}, resulting in translation inhibition. To understand the mechanisms that control de novo protein synthesis in IBV-infected cells, the expression and phosphorylation of eIF-2α in IBV-infected Vero cells were examined in detailed time course experiments. Total cell lysates were resolved with SDS-PAGE and probed with an antibody specific for p-eIF-2α at the serine 51 position and an anti-eIF-2α antibody. It showed that in IBV-infected Vero cells, p-eIF-2α was dramatically decreased after 8 h p.i. (Fig. 2a, lanes 4 to 8). The total eIF-2α remained largely stable during IBV infection in Vero cells, although a gradual decrease of the protein in this experiment and repeated experiments was observed after normalization with the tubulin loading control (Fig. 2a). The relative levels of p-eIF-2α and eIF-2α were determined by measuring the density of each band by densitometry, and the calculated ratios of p-eIF-2α to total eIF-2α are 0.64, 0.60, 0.04, 0.03, 0.03, 0.02, and 0.01 at 4, 8, 12, 16, 20, 24, and 28 h p.i., respectively. Interestingly, a specific band migrating slightly more rapidly than the eIF-2α band was detected from 12 h p.i. onwards (Fig. 2a). The identity of this band is currently unknown. It may represent a cleaved/degraded form of eIF-2α. This observation, combined with the low level of host proteins labeled at a late stage of virus infection, suggested that protein degradation might take place at these time points. For a control for the efficiency of IBV infection, the same membrane was probed with anti-IBV M antibodies, indicating a gradual increase in virus infection over time (Fig. 2a).

A similar analysis was conducted with IBV-infected HUH7 and H1299 cells, revealing a similar profile of eIF-2α expression and phosphorylation. Levels of p-eIF-2α dropped significantly from 8 h p.i. onwards (Fig. 2a, lanes 3 to 8). Subsequently, it became barely detectable, especially at 24 and 28 h p.i. (Fig. 2a, lanes 7 and 8). The ratios of p-eIF-2α to total eIF-2α in HUH7 cells are 0.28, 0.40, 0.11, 0.04, 0.03, 0.03, 0.02, and 0.003 at 0, 4, 8, 12, 16, 20, 24, and 28 h p.i., respectively. The ratios for H1299 cells are 0.10, 0.14, 0.15, 0.08, 0.008, 0.007, 0.005, and 0.002 at 0, 4, 8, 12, 16, 20, 24, and 28 h p.i., respectively. Once again, detection of the IBV M protein was carried out for an indication of IBV infection in the two cell types, showing gradually increased viral infection over time (Fig. 2a). Due to the loading of a large amount of samples for protein analysis in this experiment and prolonged exposure time, a relatively high level of p-eIF-2α was detected in both cell lines at 0 h p.i. In fact, a high basal level of p-eIF-2α was also detected in other studies (12, 41).

To further verify the results, a parallel experiment was conducted with H1299 cells incubated with UV-inactivated IBV. As shown in Fig. 2a, the basal phosphorylation levels of eIF-2α in cells infected with live IBV and UV-inactivated IBV (UV-IBV) at 0 h were similar. In contrast to that in IBV-infected cells, the p-eIF-2α level in cells incubated with UV-IBV was slightly elevated and then maintained at a stable level (Fig. 2a). This slightly increased detection of p-eIF-2α may be due to serum starvation. The absence of M protein expression in cells incubated with UV-IBV confirmed total inactivation of the virus (Fig. 2a).

To investigate the role of eIF-2α phosphorylation on IBV infection, three constructs, encoding the wild type, a nonphosphorylatable mutant (S51A), and a mutant phosphomimetic eIF-2α (S51D), were transiently expressed in H1299 cells. Cells were then infected with IBV-Luc, a recombinant IBV express-

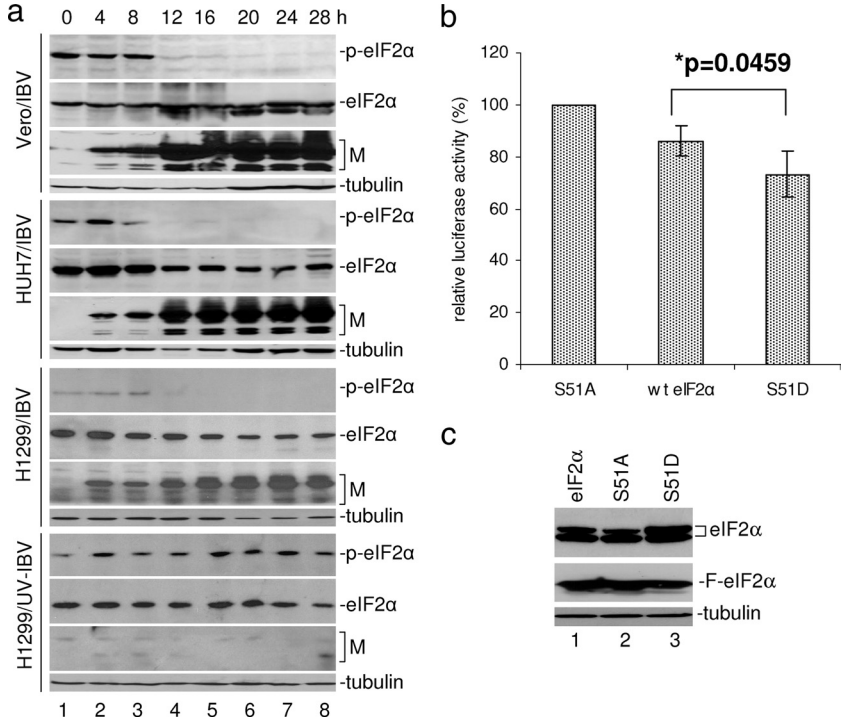

FIG. 2. Analysis of eIF-2α phosphorylation and its effect on IBV replication in IBV-infected Vero, H1299, and HUH7 cells. (a) Vero, H1299, and HUH7 cells infected with IBV at an MOI of approximately 2 were harvested and lysed at 0, 4, 8, 12, 16, 20, 24, and 28 h p.i. Lysates were separated on an SDS–12% polyacrylamide gel and examined by Western blotting using antibodies against p-eIF-2α, total eIF-2α, IBV M protein, and β-tubulin. H1299 cells were also infected with an equal amount of UV-IBV. Protein samples were separated on an SDS–12% polyacrylamide gel and probed with antibodies against p-eIF-2α (S51), total eIF-2α, IBV M protein, and β-tubulin. (b) H1299 cells were transfected with wild-type (wt) eIF-2α and its two mutants (S51A and S51D) for 16 h before infection with the recombinant IBV-Luc virus at an MOI of approximately 1. Cells were lysed in 1× PLB at 18 h p.i. and subjected to a firefly luciferase assay. The relative luciferase activity in cells expressing the S51A mutant was considered as 100%. Error bars indicate the SDs of the means from triplicate experiments. The asterisk indicates a *P* value corresponding to the difference between readings of wt eIF-2α and the S51D mutant (0.0459). (c) The same cell lysates were resolved on an SDS–12% polyacrylamide gel and examined by Western blotting using antibodies against total eIF-2α (top panel), Flag tag (F-eIF2α; middle panel), and β-tubulin (bottom panel).

ing the firefly luciferase. The relative luciferase activity represents viral subgenomic RNA synthesis and protein translation (48). The phosphorylation site is abolished in the S51A mutant and is expected to facilitate translation. The S51D mutant is a phosphomimetic mutant with a high affinity to eIF-2B, rendering translational inhibition. As shown in Fig. 2b, expression of the S51D mutant resulted in translation inhibition and suppression of viral infection. On the contrary, overexpression of the S51A mutant promoted translation and viral infection. As shown in Fig. 2b, the luciferase activity in cells expressing the S51A mutant was higher than that in cells transfected with wild-type eIF-2α. Overexpression of the wild type and the S51D mutant led to approximately 10 and 20% reductions in the luciferase activity, respectively (Fig. 2b). Comparable expression levels of the wild-type and mutant eIF-2α proteins were detected (Fig. 2c). Taken together, these data suggest that eIF-2α phosphorylation has an inhibitory effect on IBV infection and that eIF-2α is a target of IBV.

PKR phosphorylation was inhibited in IBV-infected Vero and H1299 cells, and IBV replication was regulated by overexpression of wild-type and mutant PKR. As PKR is one of the main kinases that phosphorylates eIF-2α and is a major target of many viruses to counteract host cell defense mechanisms, the expression and autophosphorylation status of PKR in IBV-infected H1299 cells were then investigated. The virus-infected cells were harvested at 0, 4, 8, 12, 16, and 20 h p.i., and total proteins were separated with SDS-PAGE. Western blotting analysis with anti-PKR antibodies showed that in IBV-infected H1299 cells, a relatively steady level of PKR was observed (Fig. 3a). When probing with anti-p-PKR antibody, p-PKR was detected as a doublet, with high basal levels at 0 and 4 h p.i. (Fig. 3a), due to the loading of large amounts of samples and prolonged exposure of the gel. There was a great reduction in the bands detected at later time points (Fig. 3a), suggesting that PKR phosphorylation was suppressed in IBV-infected cells. This observation was further supported by incubation of H1299 cells with UV-IBV. As shown in Fig. 3a, the p-PKR level remained constant. It was noted that a slightly increased level of IBV M protein was detected at some time points after prolonged exposure of the gel (Fig. 3a), probably due to incomplete inactivation of the virus in this experiment.

To further confirm the observation, both H1299 and Vero cells were infected with IBV and harvested at 0, 8, 16, 24, 36, and 48 h p.i. Western blotting analysis with anti-p-PKR antibody showed a gradual reduction of the species to an undetectable level over time in both Vero and H1299 cells, although a steady level of total PKR was detected over the time course experiments (Fig. 3b).

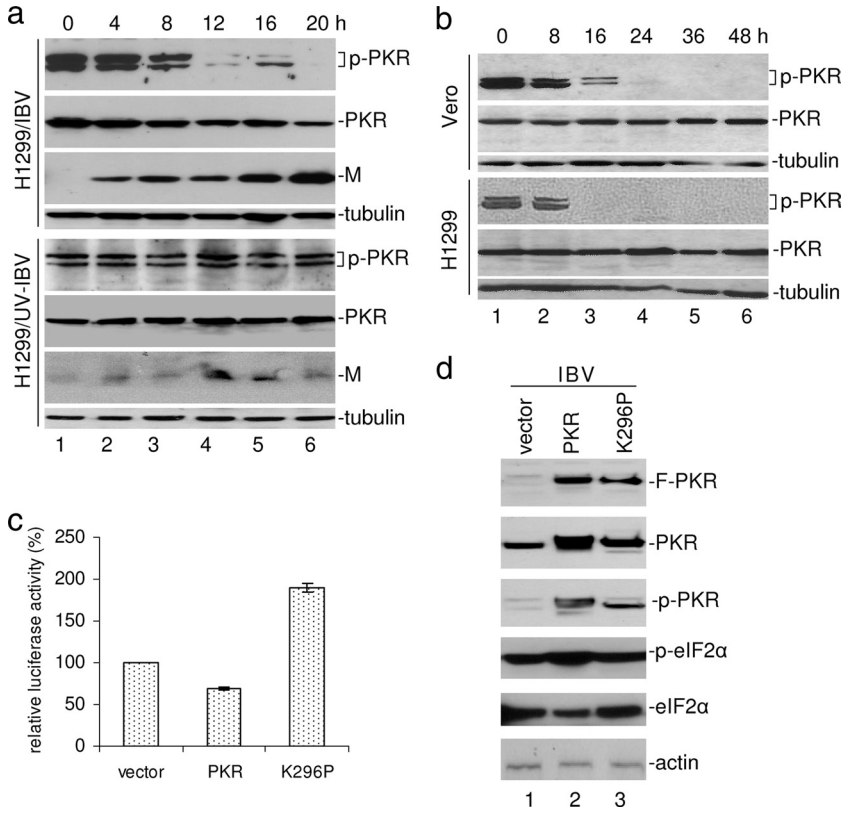

FIG. 3. Analysis of PKR phosphorylation and its effect on IBV replication in IBV-infected Vero and H1299 cells. (a) H1299 cells were infected with either IBV at an MOI of 1 or an equal amount of UV-inactivated virus and harvested at 0, 4, 8, 12, 16, and 20 h p.i. Protein samples were separated on an SDS–10% polyacrylamide gel and probed with antibodies against p-PKR (Thr451), total PKR, and β-tubulin. (b) Vero and H1299 cells were infected with IBV at an MOI of approximately 2 for 0, 8, 16, 24, 36, and 48 h before lysis. Cell lysates were separated on an SDS–12% polyacrylamide gel and examined by Western blotting with antibodies against p-PKR (Thr451), total PKR, and β-tubulin. (c) H1299 cells were transfected with wild-type PKR and the K296P mutant for 16 h before being infected with the recombinant IBV-Luc at an MOI of approximately 1. Cells were lysed in 1× PLB at 18 h p.i. and subject to a firefly luciferase assay. The relative luciferase activity in cells expressing empty vector was considered as 100%. Error bars indicate SDs of the means from triplicate experiments. (d) The same cell lysates from panel c were resolved on an SDS–10% polyacrylamide gel and examined by Western blotting with antibodies against Flag (top panel), total PKR (second panel), p-PKR (third panel), p-eIF-2α (fourth panel), total eIF-2α (fifth panel), and β-actin (bottom panel).

In order to study the effect of phosphorylation status of PKR on IBV infection, we made and expressed Flag-tagged wild type and a nonphosphorylatable mutant PKR (K296P). Overexpression of wild-type PKR in H1299 cells resulted in a 40% reduction in IBV infection, as indicated by the firefly luciferase activity (Fig. 3c). The inactive PKR K296P mutant was shown to enhance IBV infection (Fig. 3c). Western blotting analysis confirmed the overexpression of proteins by using an anti-Flag antibody (Fig. 3d, top panel). The PKR and p-PKR antibodies detected both endogenous and Flag-tagged PKRs (Fig. 3d, second and third panels from the top). As expected, more p-PKR was detected in cells overexpressing wild-type PKR (Fig. 3d, third panel) than in those expressing the K296P mutant. Furthermore, overexpression of PKR slightly induced eIF-2α phosphorylation, while less p-eIF-2α was detected in cells expressing the K296P mutant (Fig. 3d, fourth and fifth panels, lanes 2 and 3). These data further support the concept that eIF-2α phosphorylation and PKR activation regulate IBV replication.

nsp2 of IBV is a weak PKR antagonist. To further study the mechanism exploited by IBV to inhibit PKR activation, we examined the inhibitory effects of individual IBV proteins. H1299-RL cells were cotransfected with PKR, individual IBV proteins (28–30, 37–39), and a firefly luciferase reporter plasmid. We tested all IBV nsps and structural proteins except nsp3, nsp4, and nsp6, as no expression of these proteins was achieved in the overexpression system used. Figure 4a shows representative data from repeated experiments. Translation efficiency was normalized to *Renilla* luciferase readings. Overexpression of PKR resulted in a significant reduction of the translation efficiency (approximately 38%) compared to that of the vector control (Fig. 4a). Among all IBV proteins examined, only nsp2 showed restoration of the translation efficiency, to approximately 53% ($P = 0.0128$) (Fig. 4a).

To confirm the effect of nsp2 on PKR-induced translation inhibition, a dose-dependent expression experiment was performed. The influenza A virus NS1 protein, known as a PKR antagonist, was used as a control. As shown in Fig. 4b, expression of nsp2 was able to restore translation in a dose-dependent manner. When a high concentration (4 μg) of nsp2 plasmid was transfected, the translation efficiency was restored to nearly 100%, relative to that of the vector control (Fig. 4b).

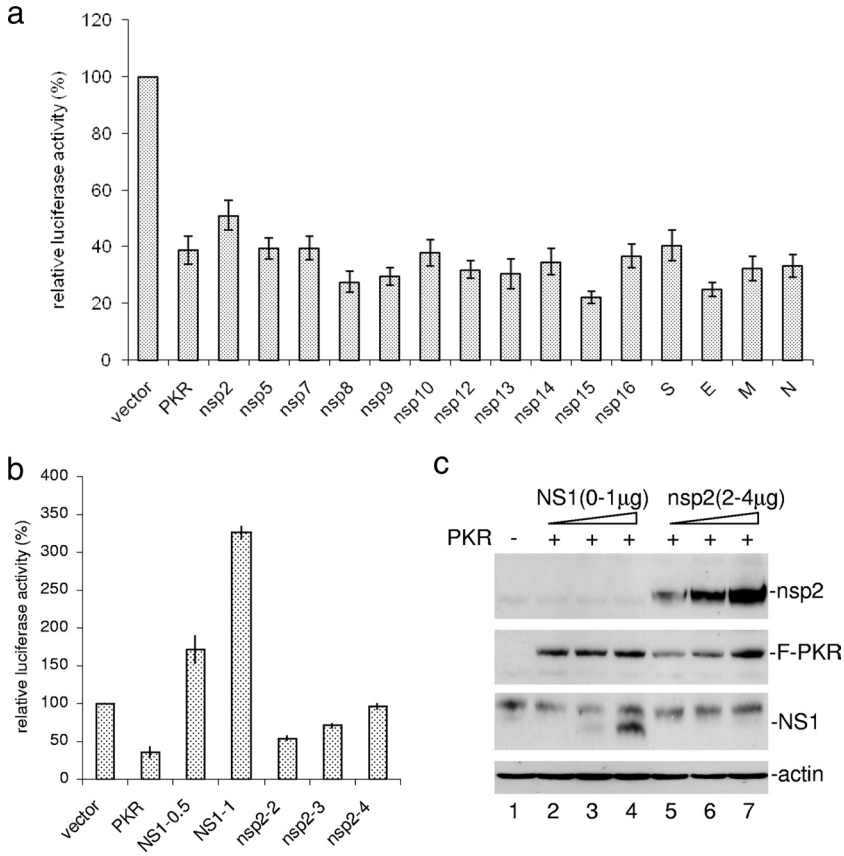

FIG. 4. Restoration of PKR-mediated translation inhibition by IBV nsp2 protein. (a) H1299-RL cells were cotransfected with 0.5 μg firefly luciferase reporter plasmid, 1 μg PKR, and 2 μg of individual IBV proteins except nsp3, nsp4, and nsp6. All constructs except the reporter plasmid carried a Flag tag. An empty vector was used as a negative control to make the total DNA amounts equal for each transfection reaction (3.5 μg). At 18 h posttransfection, cells were lysed in 200 μl 1× PLB and subjected to a dual-luciferase assay. The dual-luciferase assay was carried out using a dual-luciferase assay kit (Promega). The firefly luciferase readings were normalized against *Renilla* luciferase readings, and the translation efficiency of reporter plasmid was considered as 100% in samples expressing the firefly luciferase only (vector). Error bars indicate SDs of the means from triplicate readings. S, spike protein; E, envelope protein. (b) IBV nsp2 and influenza A virus NS1 restored translation in a dose-dependent manner. H1299-RL cells were transfected with 0.5 μg pcDNA-FL, 1 μg PKR, and different amounts of NS1 or nsp2 plasmids (listed in micrograms) by use of Lipofectamine 2000 for 18 h before lysis in 1× PLB. The total amount of DNA in each transfection was kept constant by adding different amounts of the empty vector. The dual-luciferase assay was carried out using a dual-luciferase assay kit (Promega). The firefly luciferase readings were normalized against *Renilla* luciferase readings and the translation efficiency of reporter plasmid was considered as 100% in samples expressing the firefly luciferase only (vector). Values represent means ± SDs from triplicate experiments. (c) Cell lysates were separated on a SDS–10% polyacrylamide gel and detected by Western blotting with antibodies against Flag and β-actin.

Transfection of a low concentration of the NS1 plasmid (0.5 μg) was able to restore translation to over 150% (Fig. 4b), suggesting that IBV nsp2 protein may be a weak PKR antagonist. Western blotting confirmed the expression levels of PKR, NS1, and nsp2 (Fig. 4c).

GADD34 at both mRNA and protein levels was upregulated in IBV-infected Vero, H1299, and HUH7 cells. The observation of rapid dephosphorylation of eIF-2α in IBV-infected cells prompted us to examine the expression of GADD34. Vero, H1299, and HUH7 cells were infected with either live IBV or UV-IBV in time course experiments, and Northern blotting analysis was carried out. The expression of GADD34 at the mRNA level was induced at 12 h p.i. in all three cell lines and peaked at 20 h p.i. in Vero cells and 16 h p.i. in H1299 cells and HUH7 cells (Fig. 5a, lanes 1 to 7). At 28 h p.i., both GADD34 mRNA and the 28S rRNA were found to be degraded (Fig. 5a, lane 8). However, GADD34 at the mRNA level remained unchanged in cells infected with UV-IBV throughout the time course experiments (Fig. 5a, lanes 9 to 16). Quantification of the expression of GADD34 at the mRNA level by an Affymetrix array and real-time reverse transcription-PCR in independent experiments showed 12- to 14-fold induction of the GADD34 gene in IBV-infected Vero cells at 24 h p.i. Western blotting analysis of Vero cells infected with IBV was then carried out to check the induction of GADD34 at the protein level, showing induction of GADD34 from 12 h p.i. onwards (Fig. 5b, lanes 4 and 5). At 16 h p.i., a roughly fourfold induction of the protein was observed (Fig. 5b, lane 5).

IBV replication was regulated by manipulation of GADD34 expression in virus-infected cells. To further study the functional role of GADD34 induction in IBV infection, GADD34 was transiently overexpressed in H1299 and HUH7 cells, respectively, followed by infection with the recombinant IBV-Luc virus at an MOI of approximately 1 at 12 h posttransfec-

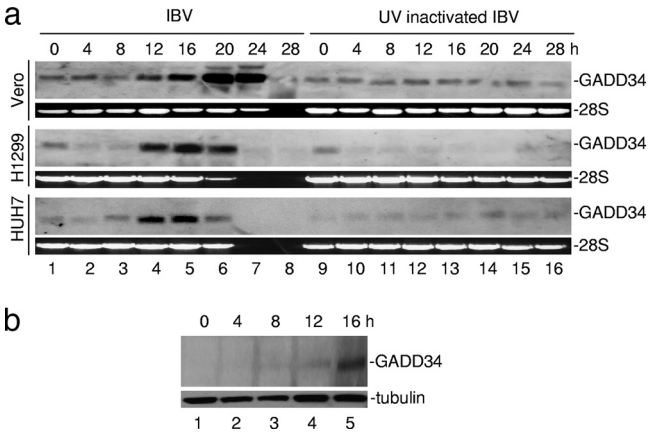

FIG. 5. Induction of GADD34 expression at mRNA and protein levels in IBV-infected Vero, H1299, and HUH7 cells. (a) Vero, H1299, and HUH7 cells were infected with live IBV at an MOI of approximately 2 or UV-IBV for 0, 4, 8, 12, 16, 20, 24, and 28 h. Total RNA was extracted and separated on an 0.9% agarose gel and examined by Northern blotting using probes for GADD34. 28S rRNA was used as a loading control. (b) H1299 cells infected with IBV at an MOI of approximately 2 for 0, 4, 8, 12, and 16 h were lysed, and total proteins were separated on an SDS–8% polyacrylamide gel. Western blotting was carried out with antibodies against GADD34 and β-tubulin.

tion. The effect of GADD34 overexpression on IBV replication was monitored by measuring the firefly luciferase activity. In both H1299 and HUH7 cells, the luciferase activity was enhanced by two- to threefold with GADD34 overexpression at 14 h p.i. (Fig. 6a, upper panel). At 16 h p.i., the luciferase activity was greatly reduced in H1299 cells, due to the death of some IBV-infected H1299 cells at this time point. Overexpression of GADD34 was confirmed by Western blotting analysis (Fig. 6a, lower panel). No GADD34 expression was detected in samples transfected with empty vector and mock infected (Fig. 6a, lower panel, lane 1) as well as in samples harvested at 0 h p.i. (Fig. 6a, lower panel, lane 2). This is probably due to a low level of endogenous GADD34 expression and inadequate plasmid expression at 12 h posttransfection. Overexpression of GADD34 resulted in dephosphorylation of eIF-2α in both cell lines (Fig. 6a, lower panels). With the increased level of GADD34, phosphorylation of eIF-2α was decreased, while the total eIF-2α remained constant (Fig. 6a, lower panels).

The effect of GADD34 knockdown on the replication of IBV was subsequently analyzed in stable cell clones expressing hairpin RNA targeting the GADD34 mRNA. Two individual G418-resistant clones with efficient GADD34 knockdown were selected and confirmed by Western blotting analysis. As shown in Fig. 6b (upper panels), significant reduction of GADD34 expression at the protein level was observed in clone 2. Com-

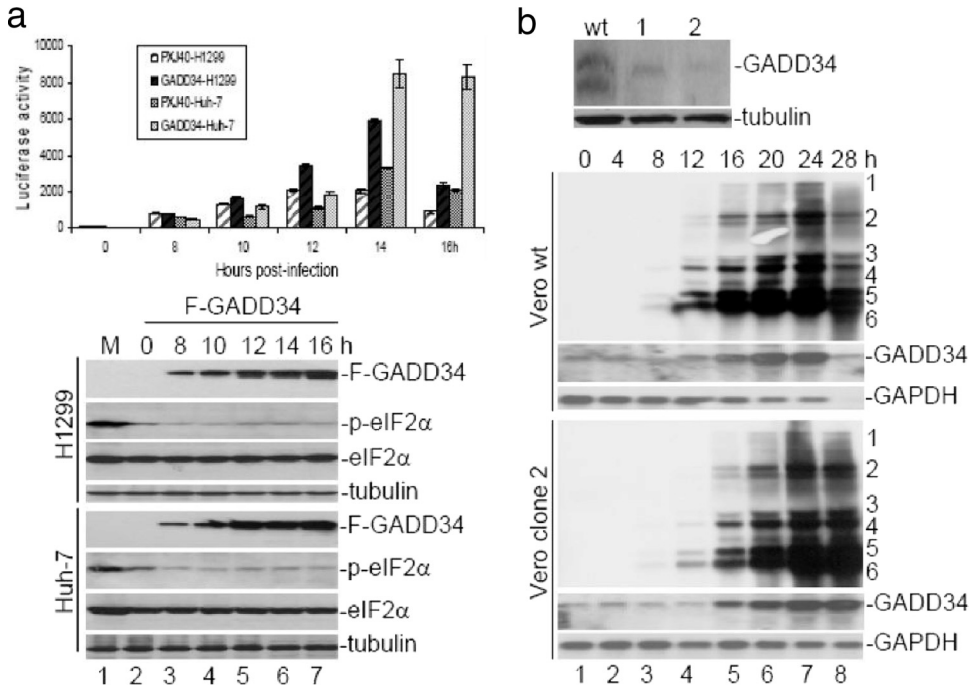

FIG. 6. Regulation of IBV replication by manipulation of GADD34 expression. (a) Facilitation of IBV replication by overexpression of GADD34 in HUH7 and H1299. (Upper panel) H1299 and HUH7 cells were transfected with pXJ40F-GADD34 (F-GADD34) or the empty vector for 12 h before infection with the recombinant IBV-Luc virus at an MOI of approximately 1 for 0, 8, 10, 12, 14, and 16 h before lysis in 1× PLB. Luciferase assay was carried out using a luciferase assay kit from Promega. Error bars indicate means ± SDs from triplicate experiments. (Lower panel) Proteins from the same lysates were resolved with 10% SDS-PAGE and examined by Western blotting with antibodies against GADD34, p-eIF-2α, total eIF-2α, and β-tubulin. M, cells transfected with empty vector and mock infected for 16 h before lysis. (b) GADD34 knockdown facilitated virus infection. Vero cells were stably transfected with short hairpin RNA of GADD34, and two knockdown clones were selected and examined by Western blotting (upper panel). Vero GADD34 knockdown cells (clone 2) and wild-type (wt) cells were infected with IBV for 0, 4, 8, 12, 16, 20, 24, and 28 h before RNA extraction. Equal amounts of total RNAs were separated on a 0.9% agarose gel and examined by Northern blotting using probes for IBV, GADD34, and GAPDH. The six RNA species of IBV are indicated on the right of the gels.

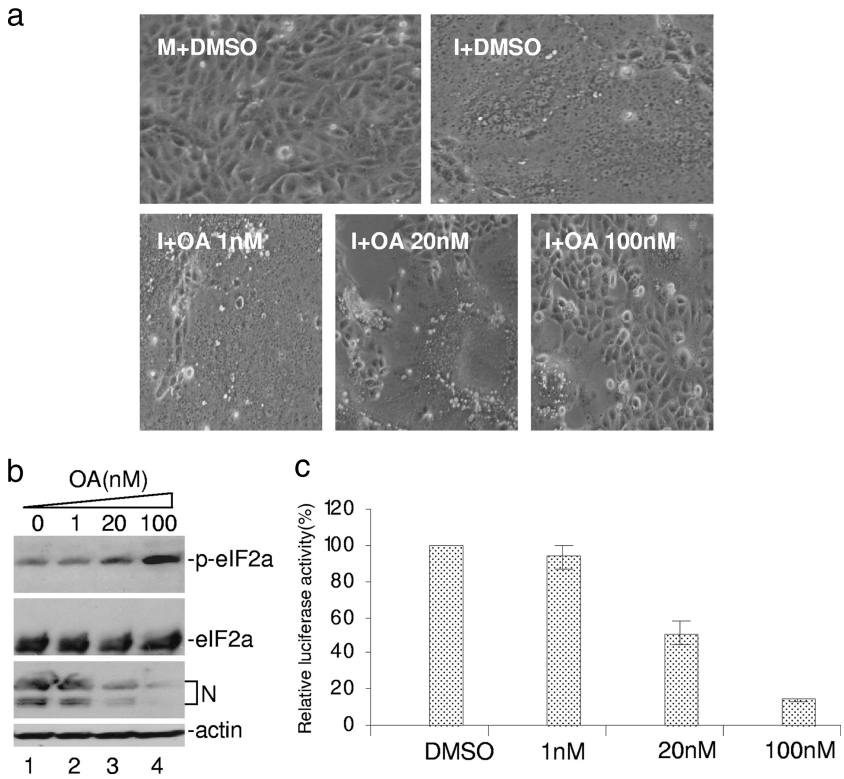

FIG. 7. Reduction of IBV replication by inhibition of the PP1 activity with OA in IBV-infected Vero cells. (a) Light microscopy images of IBV-infected Vero cells either untreated or treated with different concentrations of OA. Vero cells were treated with DMSO or OA 1 h after infection with IBV-Luc. Images were taken at 18 h p.i. M, mock infection; I, IBV infection. (b) Cells from the experiment described above were harvested at 18 h p.i. Total proteins were resolved on an SDS–12% polyacrylamide gel and examined by Western blotting with antibodies against p-eIF-2α, total eIF-2α, IBV N, and β-tubulin. (c) Cell lysates were subjected to a luciferase activity assay. IBV infection in cells treated with DMSO was considered as 100%. Error bars indicate SDs of the means of triplicate experiments.

pared to the case for wild-type IBV-infected cells, a reduced and delayed induction of GADD34 in knockdown cells infected with IBV was observed, as shown in Northern blotting analysis (Fig. 6b, lower panels, lanes 1 to 6). Quantitative data showed that the level of GADD34 at 0 h p.i. in knockdown cells was 30% of that in wild-type Vero cells. In wild-type Vero cells, GADD34 expression increased by 3.8-fold at 12 h p.i. In contrast, GADD34 expression in knockdown cells increased by 0.63-fold at the same time point, and a 3-fold induction was achieved only at 20 h p.i. At 28 h p.i., a high level of GADD34 induction remained detectable in IBV-infected GADD34 knockdown cells, but much less GADD34 was detected in IBV-infected wild-type cells (Fig. 6b, lower panels, lane 8). As only a trace amount of GAPDH (glyceraldehyde-3-phosphate dehydrogenase) was detected in IBV-infected wild-type cells at this time point, the reduction of detected GADD34 is probably due to cell death and RNA degradation as described previously. Densitometry data showed that GADD34 expression was induced 13-fold in wild-type cells, but only 6.3-fold induction was observed in knockdown cells. Northern blotting analysis of IBV RNA showed significantly reduced replication of viral RNA from 8 to 20 h p.i. in GADD34 knockdown cells infected with IBV, compared to IBV-infected wild-type cells (Fig. 6b, lower panels, lanes 1 to 6). Efficient replication of viral RNA was observed in both types of cells at 24 h p.i. (Fig. 6b, lower panels, lane 7). Interestingly, the level of viral RNA replication that remained detectable at 28 h p.i. in IBV-infected GADD34 knockdown cells was much higher than that in wild-type cells (Fig. 6b, lower panels, lane 8), suggesting that knockdown of GADD34 delayed the replication of IBV.

IBV replication was inhibited by PP1 inhibitor OA. We next investigated the effect of PP1 activity on the replication of IBV by using OA, a potent inhibitor of PP1 and PP2A. OA selectively inhibits PP2A activity at low concentrations (50% inhibitory concentration, ~0.1 nM) and both PP1 and PP2A activities at high concentrations (50% inhibitory concentration for PP1, ~20 nM) (11, 35). Vero cells were incubated in the presence of OA or DMSO at 1 h p.i. and harvested at 18 h p.i., and cell lysates were analyzed by Western blotting. When treated with DMSO alone, the infected cells showed a massive formation of syncytia, a typical cytopathic effect of IBV infection (Fig. 7a, panel I+DMSO). In IBV-infected cells treated with 1 nM OA, the degree of syncytium formation was comparable to that in DMSO-treated cells (Fig. 7a, I+OA 1 nM). In contrast, viral infection was restricted to certain areas in cells treated with 20 nM and 100 nM OA (Fig. 7a, panels I+OA 20 nM and I+OA 100 nM, respectively), suggesting that IBV infection was inhibited by OA at these concentrations. Consistently, the detected level of N protein in cells treated with 1 nM OA was comparable to that in DMSO-treated cells (Fig. 7b, lanes 1 and 2). Synthesis of the N protein was moderately inhibited in cells treated with 20 nM (Fig. 7b, lane 3)

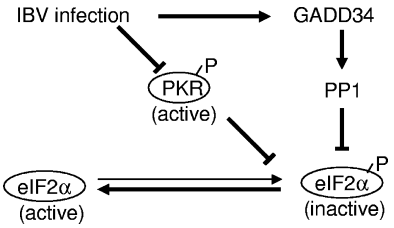

FIG. 8. Working model. A low level of de novo host cell global translation was maintained in IBV-infected cells by reducing the eIF-2α phosphorylation via a combination of two mechanisms, i.e., inhibition of PKR activation and induction of GADD34. The light arrow indicates that the reaction is less active in cells under normal circumstances.

but severely inhibited in cells treated with 100 nM OA (Fig. 7b, lane 4). As expected, the phosphorylation level of eIF-2α in cells treated with 1 nM OA was similar to that in DMSO-treated cells (Fig. 7b, lanes 1 and 2) but significantly increased in cells treated with 20 nM and 100 nM OA (Fig. 7b, lanes 3 and 4, respectively).

The effect of inhibition of the PP1 activity by OA on IBV replication was more accurately quantified by infection of Vero cells with the recombinant IBV-Luc virus. Compared to cells treated with DMSO only (considered as 100% infection), IBV infection was reduced to approximately 92, 55, and 10% in cells treated with 1, 20, and 100 nM of OA, respectively (Fig. 7c). Taken together, these results demonstrated that suppression of the PP1 activity, but not the PP2A activity, rendered an inhibitory effect on IBV replication, indicating that OA may inhibit IBV infection via inhibition of the host translation machinery, specifically, by elevating the eIF-2α phosphorylation level.

DISCUSSION

As obligatory intracellular parasites, RNA viruses rely solely on host cell translation machinery for synthesis of their structural and functional components. Many viruses have therefore evolved a diversity of regulatory mechanisms to modulate host protein synthesis in order to maximize the production of progeny viruses (44). One of the most extensively studied pathways that modulates viral and host cell protein synthesis in many viral systems is the phosphorylation/dephosphorylation of eIF-2α (50). Modulation of this pathway usually results in preferential expression of viral gene products (10). In this study, we show that the basal level of phosphorylated eIF-2α was rapidly reduced, via induction of GADD34 expression and inhibition of PKR autophosphorylation, in cells infected with the coronavirus IBV at early stages of the infection cycle (Fig. 8). Meanwhile, IBV infection led to a slight reduction of the total eIF-2α, possibly through an unidentified virus-mediated cleavage/degradation mechanism. Consequently, de novo synthesis of host proteins remains functionally active, although at a relatively low level.

A minimal to moderate reduction of de novo synthesis of host proteins was detected in IBV-infected cells at late stages of the infection cycle even when p-eIF-2α was dramatically reduced. Several possibilities were considered. First, the observed slightly lower level of global translation at late stages of virus infection is possibly due to the relatively poor labeling of host proteins at 16 and 24 h p.i. At these stages, a certain proportion of the infected cells is dead and starts to detach from the culture dishes, making it difficult to metabolically label these dead/dying cells. It would be reasonable to speculate that more active de novo synthesis of host proteins than that reflected by the metabolic labeling might be actually taking place. Nevertheless, the steady level of total host proteins was minimally affected in the infected cells compared to the controls at each time points. Second, the overall level of total eIF-2α was appreciably reduced in IBV-infected cells at late stages of the infection cycle. As viral mRNAs accumulate to a high level in the infected cells at these time points, the reduction of total eIF-2α would render a preferential inhibitory effect on the overall synthesis of host proteins. Third, additional virus-induced mechanisms may preferentially inhibit host cell gene expression. For example, degradation of the host RNAs, including mRNA and rRNA, is observed in IBV-infected cells at these stages of the infection cycle. This would result in the reduction of host protein synthesis. The abundant 28S rRNA and mRNA for the housekeeping GAPDH gene were found to be reduced to undetectable levels in IBV-infected Vero cells at 28 h p.i. In IBV-infected H1299 and HUH7 cells, degradation of these RNA species was observed as early as 24 h p.i., reflecting the fact that IBV has more rapid replication and shorter infection cycles in these two cell lines. Finally, virus may encode an element(s) that interferes with other translation factors. A good example is that protein translation was inhibited in cells expressing IBV spike protein, via the interaction with eIF3f (55).

In cells infected with IBV, six mRNA species, including the 27.6-kb genome-length mRNA1 and five subgenome-length mRNAs, mRNA2 to mRNA6, are produced (26). It is generally believed that these mRNA species are capped at the 5′ end and polyadenylated at the 3′ end. Translation of them would thus follow the canonical rules governing translation of cellular mRNAs, although alternative mechanisms may also be used by some of these mRNA species (28, 29, 32, 40, 56). Therefore, it is not surprising that phosphorylation of eIF-2α may have an adverse effect on IBV infection. This was supported by the data that indicated that overexpression of a nonphosphorylated-eIF-2α mutant favored IBV infection. However, the observations that IBV infection in cell culture led to the inhibition of eIF-2α phosphorylation and PKR activation are contradictory to a recent study with severe acute respiratory syndrome (SARS) coronavirus, showing that SARS coronavirus infection enhances the phosphorylation of eIF-2α and PKR (20). Inconsistent data were also reported for murine hepatitis virus (MHV) strain A59. In cells infected with MHV A59, PKR and eIF-2α were shown not to be phosphorylated, and little reduction of overall protein translation was observed (57). In a more recent study, however, eIF-2α phosphorylation was shown to be reduced within 6 h p.i. but induced at 8 h p.i. in cells infected with MHV A59 (3). Furthermore, the expression of GADD34 was not affected, resulting in a sustained suppression of host protein translation (3). It was also suggested that suppression of global translation in MHV-infected cells may result from 28S rRNA cleavage (2), which was not observed in IBV-infected cells. The reasons for these controversial observations are not fully understood. One possibility is the lack of nsp1 protein in IBV, as nsp1 may be involved in regulation of host

cell translation by either modulation of the phosphorylation of eIF-2α or stress granule formation (3). These differences, on the other hand, reflect the complexity of virus-host interactions even among members of the same viral family.

PKR is normally present in cells in a latent state. Upon activation by dsRNA, PKR is autophosphorylated and forms a dimer. The activated PKR phosphorylates eIF-2α at the Ser51 residue and results in shutdown of protein translation (15). In cells infected with other coronaviruses, additional eIF-2α kinases were reported to be activated. For example, PERK was shown to be activated in cells infected with SARS coronavirus (20), leading to eIF-2α phosphorylation. In cells infected with IBV, detection of PERK activation was not successful (data not shown). Viruses have evolved multiple mechanisms to block the PKR response in various steps of the pathway (10). For example, many viruses encode dsRNA-binding proteins, such as the vaccinia virus E3L protein, resulting in the inhibition of PKR activation (6). Coronaviruses code for a number of dsRNA-binding proteins, including several nsps derived from the replicase genes (58). In this study, efforts were made to identify the viral components involved in inactivation of PKR. Among all the proteins tested, only nsp2 showed its ability in restoring translation efficiency. Graham et al. (12) showed that MHV and SARS coronavirus mutants with a deletion of nsp2 affected RNA synthesis, but nsp2 was not required for viral replication. The role of nsp2 during viral infection remains to be elucidated.

Based on the observations that IBV-induced GADD34 expression corresponds to the phosphorylation status of eIF-2α and overexpression of GADD34 facilitates IBV infection, probably via promotion of protein translation, it is concluded that GADD34 may play a key role in regulation of eIF-2α phosphorylation in IBV-infected cells. To our knowledge, there was no report so far that infection of cells with other coronaviruses led to upregulation of GADD34. It appears that this regulation mechanism is a unique feature in IBV infection. Attempts to identify individual IBV proteins responsible for this upregulation were made but were unsuccessful. When individual IBV proteins were overexpressed in cells, no induction of GADD34 was detected (unpublished observations). As MHV infection does not induce GADD34 expression (3), induction of an unfolded protein response in virus-infected cells is unlikely the sole mechanism underlying IBV-induced GADD34 expression. It appears that multiple cellular pathways and viral components may be involved. This would be an interesting topic for further studies.

REFERENCES

1. **Aggen, J. B., A. C. Nairn, and R. Chamberlin.** 2000. Regulation of protein phosphatase-1. Chem. Biol. **7:**R13–R23.
2. **Banerjee, S., S. An, A. Zhou, R. H. Silverman, and S. Makino.** 2000. RNase L-independent specific 28S rRNA cleavage in murine coronavirus-infected cells. J. Virol. **74:**8793–8802.
3. **Bechill, J., Z. Chen, J. W. Brewer, and S. C. Baker.** 2008. Coronavirus infection modulates the unfolded protein response and mediates sustained translational repression. J. Virol. **82:**4492–4501.
4. **Brush, M. H., D. C. Weiser, and S. Shenolikar.** 2003. Growth arrest and DNA damage-inducible protein GADD34 targets protein phosphatase 1α to the endoplasmic reticulum and promotes dephosphorylation of the alpha subunit of eukaryotic translation initiation factor 2. Mol. Cell. Biol. **23:**1292–1303.
5. **Cassady, K. A., M. Gross, and B. Roizman.** 1998. The second-site mutation in the herpes simplex virus recombinants lacking the γ134.5 genes precludes shutoff of protein synthesis by blocking the phosphorylation of eIF-2α. J. Virol. **72:**7005–7011.
6. **Chang, H. W., J. C. Watson, and B. L. Jacobs.** 1992. The E3L gene of vaccinia virus encodes an inhibitor of the interferon-induced, double-stranded RNA-dependent protein kinase. Proc. Natl. Acad. Sci. USA **89:**4825–4829.
7. **Chen, J. J.** 2000. Heme-regulated eIF-2α kinase, p. 529–546. *In* N. Sonenberg, J. W. B. Hershey, and M. B. Mathews (ed.), Translational control of gene expression. Cold Spring Harbor Laboratory Press, Cold Spring Harbor, NY.
8. **Cohen, P. T. W.** 2002. Protein phosphatase 1—targeted in many directions. J. Cell Sci. **115:**241–256.
9. **Dever, T. E.** 2002. Gene-specific regulation by general translation factors. Cell **108:**545–556.
10. **Gale, M. Jr., S. L. Tan, and M. G. Katze.** 2000. Translational control of viral gene expression in eukaryotes. Microbiol. Mol. Biol. Rev. **64:**239–280.
11. **Garcia, A., X. Cayla, J. Guergnon, F. Dessauge, V. Hospital, M. P. Rebollo, A. Fleischer, and A. Rebollo.** 2003. Serine/threonine protein phosphatases PP1 and PP2A are key players in apoptosis. Biochimie **85:**721–726.
12. **Graham, R. L., A. C. Sims, S. M. Brockway, R. S. Barics, and M. R. Denison.** 2005. The nsp2 replicase proteins of murine hepatitis virus and severe acute respiratory syndrome coronavirus are dispensable for viral replication. J. Virol. **79:**13399–13411.
13. **Hebner, C. M., R. Wilson, J. Rader, M. Bidder, and L. A. Laimins.** 2006. Human papillomaviruses target the double-stranded RNA protein kinase pathway. J. Gen. Virol. **87:**3188–3193.
14. **Hinnebusch, A. G.** 2000. Mechanism and regulation of initiator methionyl-tRNA binding to ribosomes, p. 185–244. *In* N. Sonenberg, J. W. Hershey, and M. B. Mathews (ed.), Translational control of gene expression. Cold Spring Harbor Laboratory Press, Cold Spring Harbor, NY.
15. **Hovanessian, A. G.** 1989. The double stranded RNA-activated protein kinase induced by interferon: dsRNA-PK. J. Interferon Res. **9:**641–647.
16. **Katze, M. G.** 1995. Regulation of the interferon-induced PKR: can viruses cope? Trends Microbiol. **3:**75–78.
17. **Katze, M. G., Y. He, and M. Gale, Jr.** 2002. Viruses and interferon: a fight for supremacy. Nat. Rev. Immunol. **2:**675–687.
18. **Kazemi, S., S. Papadopoulou, S. Li, Q. Su, S. Wang, A. Yoshimura, G. Matlashewski, T. E. Dever, and A. E. Koromilas.** 2004. Control of α subunit of eukaryotic translation initiation factor 2 (eIF2α) phosphorylation by the human papillomavirus type 18 E6 oncoprotein: implications for eIF2α-dependent gene expression and cell death. Mol. Cell. Biol. **24:**3415–3429.
19. **Kimball, S. R.** 2001. Regulation of translation initiation by amino acids in eukaryotic cells. Prog. Mol. Subcell. Biol. **26:**155–184.
20. **Krähling, V., D. A. Stein, M. Spiegel, F. Weber, and E. Mühlberger.** 2009. Severe acute respiratory syndrome coronavirus triggers apoptosis via protein kinase R but is resistant to its antiviral activity. J. Virol. **83:**2298–2309.
21. **Li, S., J. Y. Min, R. M. Krug, and G. C. Sen.** 2006. Binding of the influenza A virus NS1 protein to PKR mediates the inhibition of its activation by either PACT or double-stranded RNA. Virology **349:**13–21.
22. **Lim, K. P., and D. X. Liu.** 1998. Characterization of the two overlapping papain-like proteinase domain encoded in gene 1 of the coronavirus infectious bronchitis virus and determination of the C-terminal cleavage site of an 87 kDa protein. Virology **245:**303–312.
23. **Lim, K. P., L. F. P. Ng, and D. X. Liu.** 2000. Identification of a novel cleavage activity of the first papain-like proteinase domain encoded by open reading frame 1a of the coronavirus avian infectious bronchitis virus and characterization of the cleavage products. J. Virol. **74:**1674–1685.
24. **Liu, D. X., I. Brierley, K. W. Tibbles, and T. D. K. Brown.** 1994. A 100-kilodalton polypeptide encoded by open reading frame (ORF) 1b of the coronavirus infectious bronchitis virus is processed by ORF 1a products. J. Virol. **68:**5772–5780.
25. **Liu, D. X., and T. D. K. Brown.** 1995. Characterization and mutational analysis of an ORF1a-encoding proteinase domain responsible for proteolytic processing of the infectious bronchitis virus 1a/1b polyprotein. Virology **209:**420–427.
26. **Liu, D. X., D. Cavanagh, P. Green, and S. C. Inglis.** 1991. A polycistronic mRNA specified by the coronavirus infectious bronchitis virus. Virology **184:**531–544.
27. **Liu, D. X., and S. C. Inglis.** 1991. Association of the infectious bronchitis virus 3c protein with the virion envelope. Virology **185:**911–917.
28. **Liu, D. X., and S. C. Inglis.** 1992. Internal entry of ribosomes on a tricistronic mRNA encoded by infectious bronchitis virus. J. Virol. **66:**6143–6154.
29. **Liu, D. X., and S. C. Inglis.** 1992. Identification of two new polypeptides encoded by mRNA5 of the coronavirus infectious bronchitis virus. Virology **186:**342–347.
30. **Liu, D. X., S. Shen, H. Y. Xu, and S. F. Wang.** 1998. Proteolytic mapping of the coronavirus infectious bronchitis virus 1b polyprotein: evidence for the presence of four cleavage sites of the 3C-like proteinase and identification of two novel cleavage products. Virology **246:**288–297.
31. **Liu, D. X., K. W. Tibbles, D. Cavanagh, T. D. K. Brown, and I. Brierley.** 1995. Identification, expression and processing of an 87K polypeptide encoded by ORF1a of the coronavirus infectious bronchitis virus. Virology **208:**48–54.
32. **Liu, D. X., H. Y. Xu, and T. D. K. Brown.** 1997. Proteolytic processing of the coronavirus infectious bronchitis virus 1a polyprotein: identification of a

10-kilodalton polypeptide and determination of its cleavage sites. J. Virol. **71:**1814–1820.
33. **Melville, M. W., S. L. Tan, M. Wambach, J. Song, R. I. Morimoto, and M. G. Katze.** 1999. The cellular inhibitor of the PKR protein kinase, P58 (IPK), is an influenza virus-activated co-chaperone that modulates heat shock protein 70 activity. J. Biol. Chem. **274:**3797–3803.
34. **Meurs, E., K. Chong, J. Galabru, N. S. Thomas, I. M. Kerr, B. R. Williams, and A. G. Hovanessian.** 1990. Molecular cloning and characterization of the human double-stranded RNA-activated protein kinase induced by interferon. Cell **62:**379–390.
35. **Millward, T. A., S. Zolnierowicz, and B. A. Hemmings.** 1999. Regulation of protein kinase cascades by protein phosphatase 2A. Trends Biochem. Sci. **24:**186–191.
36. **Minami, K., Y. Tambe, R. Watanabe, T. Isono, M. Haneda, K. Isobe, T. Kobayashi, O. Hino, H. Okabe, T. Chano, and H. Inoue.** 2007. Suppression of viral replication by stress-inducible GADD34 protein via the mammalian serine/threonine protein kinase mTOR pathway. J. Virol. **81:**11106–11115.
37. **Nanduri, S., F. Rahman, B. R. William, and J. Qin.** 2000. A dynamically tuned double-stranded RNA binding mechanism for the activation of antiviral kinase PKR. EMBO J. **19:**5567–5574.
38. **Ng, L. F. P., and D. X. Liu.** 1998. Identification of a 24 kDa polypeptide processed from the coronavirus infectious bronchitis virus 1a polyprotein by the 3C-like proteinase and determination of its cleavage sites. Virology **243:**388–395.
39. **Ng, L. F. P., and D. X. Liu.** 2000. Further characterization of the coronavirus infectious bronchitis virus 3C-like proteinase and determination of a new cleavage site. Virology **272:**27–39.
40. **Ng, L. F. P., and D. X. Liu.** 2002. Membrane association and dimerization of a cysteine-rich, 16-kilodalton polypeptide released from the C-terminal region of the coronavirus infectious bronchitis virus 1a polyprotein. J. Virol. **76:**6257–6267.
41. **Nie, Y., G. L. Hammond, and J. H. Yang.** 2007. Double-stranded RNA deaminase ADAR1 increases host susceptibility to virus infection. J. Virol. **81:**917–923.
42. **Novoa, I., H. Zeng, H. P. Harding, and D. Ron.** 2001. Feedback inhibition of the unfolded protein response by GADD34-mediated dephosphorylation of eIF2alpha. J. Cell Biol. **153:**1011–1022.
43. **Novoa, I., Y. Zhang, H. Zeng, R. Jungreis, H. P. Harding, and D. Ron.** 2003. Stress-induced gene expression requires programmed recovery from translational repression. EMBO J. **22:**1180–1187.
44. **Pe'ery, T., and M. B. Mathews.** 2000. Viral translational strategies and host defense mechanisms, p. 371–424. *In* N. Sonenberg, J. W. B. Hershey, and M. B. Mathews (ed.), Translational control of gene expression. Cold Spring Harbor Laboratory Press, Cold Spring Harbor, NY.
45. **Ron, D.** 2002. Translational control in the endoplasmic reticulum stress response. J. Clin. Investig. **110:**1383–1388.
46. **Samuel, C. E.** 1993. The eIF-2 alpha protein kinases, regulators of translation in eukaryotes from yeasts to humans. J. Biol. Chem. **268:**7603–7606.
47. **Schneider, R. J., and I. Mohr.** 2003. Translation initiation and viral tricks. Trends Biochem. Sci. **28:**130–136.
48. **Shen, H., S. Fang, B. Chen, G. Chen, P. L. Tay, and D. X. Liu.** 2009. Towards construction of viral vectors based on avian coronavirus infectious bronchitis virus for gene delivery and vaccine development. J. Virol. Methods **160:**48–56.
49. **Tan, S. L., and M. G. Katze.** 1998. Biochemical and genetic evidence for complex formation between the influenza A virus NS1 protein and the interferon-induced PKR protein kinase. J. Interferon Cytokine Res. **18:**757–766.
50. **Thompson, S. R., and P. Sarnow.** 2000. Regulation of host cell translation by viruses and effects on cell function. Curr. Opin. Microbiol. **3:**366–370.
51. **Ventoso, I., M. A. Sanz, S. Molina, J. J. Berlanga, L. Carrasco, and M. Esteban.** 2006. Translational resistance of late alphavirus mRNA to eIF2alpha phosphorylation: a strategy to overcome the antiviral effect of protein kinase PKR. Genes Dev. **20:**87–100.
52. **Villafranca, J. E., C. R. Kissinger, and H. E. Parge.** 1996. Protein serine/threonine phosphatases. Curr. Opin. Biotechnol. **7:**397–402.
53. **West, M. H., J. P. Trempe, J. D. Tratschin, and B. J. Carter.** 1987. Gene expression in adeno-associated virus vectors: the effects of chimeric mRNA structure, helper virus, and adenovirus VA1 RNA. Virology **160:**38–47.
54. **Williams, B. R.** 1999. PKR; a sentinel kinase for cellular stress. Oncogene **18:**6112–6120.
55. **Xiao, H., L. H. Xu, Y. Yamada, and D. X. Liu.** 2008. Coronavirus spike protein inhibits host cell translation by interaction with eIF3f. PLoS ONE **3:**e1494.
56. **Xu, H. Y., K. P. Lim, S. Shen, and D. X. Liu.** 2001. Further identification and characterization of novel intermediate- and mature-cleavage products released from the ORF 1b region of the avian coronavirus infectious bronchitis virus1a/1b polyprotein. Virology **288:**212–222.
57. **Ye, Y., K. Hauns, J. O. Langland, B. L. Jacobs, and B. G. Hogue.** 2007. Mouse hepatitis coronavirus A59 nucleocapsid protein is a type I interferon antagonist. J. Virol. **81:**2554–2563.
58. **Ziebuhr, J.** 2005. The coronavirus replicase. Curr. Top. Microbiol. Immunol. **287:**57–94.